Dilution impacts on smoke aging: Evidence in BBOP data

Anna L. Hodshire[1], Emily Ramnarine[1], Ali Akherati[2], Matthew L. Alvarado[3], Delphine K. Farmer[4], Shantanu H. Jathar[2], Sonia M. Kreidenweis[1], Chantelle R. Lonsdale[3], Timothy B. Onasch[5], Stephen R. Springston[6], Jian Wang[6,a], Yang Wang[7,b], Lawrence I. Kleinman[6], Arthur J. Sedlacek III[6], Jeffrey R. Pierce[1]

[1] Department of Atmospheric Science, Colorado State University, Fort Collins, CO 80523, United States
[2] Department of Mechanical Engineering, Colorado State University, Fort Collins, CO 80523, United States
[3] Atmospheric and Environmental Research, Inc., Lexington, MA 02421, United States
[4] Department of Chemistry, Colorado State University, Fort Collins, CO 80523, United States
[5] Aerodyne Research Inc., Billerica, MA 01821, United States
[6] Environmental and Climate Sciences Department, Brookhaven National Laboratory, Upton, NY 11973, United States
[7] Center for Aerosol Science and Engineering, Washington University, St. Louis, MO 63130, United States
[a] Now at Center for Aerosol Science and Engineering, Washington University, St. Louis, MO 63130, United States
[b] Now at Department of Civil, Architectural and Environmental Engineering, Missouri University of Science and Technology, Rolla, Missouri 65409, United States

Correspondence to: Anna L. Hodshire (Anna.Hodshire@colostate.edu)

Abstract. Biomass burning emits vapors and aerosols into the atmosphere that can rapidly evolve as smoke plumes travel downwind and dilute, affecting climate- and health-relevant properties of the smoke. To date, theory has been unable to explain variability in smoke evolution. Here, we use observational data from the BBOP field campaign and show that initial smoke concentrations can help predict changes in smoke aerosol aging markers, number, and diameter. Because initial field measurements of plumes are generally >10 minutes downwind, smaller plumes will have already undergone substantial dilution relative to larger plumes. However, the extent to which dilution has occurred prior to the first observation is not a measurable quantity. Hence, initial observed concentrations can serve as an indicator of dilution, which impacts photochemistry and aerosol evaporation. Cores of plumes have higher concentrations than edges. By segregating the observed plumes into cores and edges, we infer that particle aging, evaporation, and coagulation occurred before the first measurement, and we find that edges generally undergo higher increases in oxidation tracers, more decreases in semivolatile compounds, and less coagulation than the cores.

1 Introduction

40   Smoke from biomass burning is a major source of atmospheric primary aerosol and vapors (Akagi et al., 2011; Gilman et al., 2015; Hatch et al., 2015, 2017; Jen et al., 2019; Koss et al., 2018; Reid et al., 2005; Yokelson et al., 2009), influencing air quality, local radiation budgets, cloud properties, and climate (Carrico et al., 2008; O'Dell et al., 2019; Petters et al., 2009; Ramnarine et al., 2019; Shrivastava et al., 2017), as well as the health of smoke-impacted communities (Ford et al., 2018; Gan et al., 2017; Reid et al., 2016). Vapors and particles emitted from fires can rapidly evolve as smoke travels

45   downwind (Adachi et al., 2019; Akagi et al., 2012; Bian et al., 2017; Cubison et al., 2011; Hecobian et al., 2011; Hodshire et al., 2019a, 2019b; Jolleys et al., 2012, 2015; Konovalov et al., 2019; May et al., 2015; Noyes et al., 2020; Sakamoto et al., 2015), diluting and entraining regional background air. Fires span an immense range in size, from small agricultural burns, which may be only a few m^2 in total area and last a few hours, to massive wildfires, which may burn 10,000s of km^2 over the course of weeks (Andela et al., 2019). This range in size leads to variability in initial plume size and dilution, as large, thick

50   plumes dilute more slowly than small, thin plumes for similar atmospheric conditions (Akagi et al., 2012; Bian et al., 2017; Cubison et al., 2011; Hecobian et al., 2011; Hodshire et al., 2019a, 2019b; Jolleys et al., 2012, 2015; Konovalov et al., 2019; May et al., 2015; Sakamoto et al., 2015)). Plumes can dilute unevenly, with edges of the plume mixing in with surrounding air more rapidly than the core of the plume. Variability in dilution leads to variability in the evolution of smoke emissions as instantaneous plume thickness will control shortwave fluxes (and thus photolysis rates and oxidant concentrations), gas-

55   particle partitioning, and particle coagulation rates ((Akagi et al., 2012; Bian et al., 2017; Cubison et al., 2011; Hecobian et al., 2011; Hodshire et al., 2019a, 2019b; Jolleys et al., 2012, 2015; Konovalov et al., 2019; May et al., 2015; Sakamoto et al., 2015), (Garofalo et al., 2019), (Ramnarine et al., 2019; Sakamoto et al., 2016)). Thus, capturing variability in plume thickness and dilution between fires and within fires can aid in understanding how species change within the first few hours of emission for a range of plume sizes.

60   The evolution of total particulate matter (PM) or organic aerosol (OA) mass from smoke has been the focus of many studies, as PM influences both human health and climate. Secondary organic aerosol (SOA) production may come about through oxidation of gas-phase volatile organic compounds (VOCs) that can form lower-volatility products that partition to the condensed phase (Jimenez et al., 2009; Kroll and Seinfeld, 2008). SOA formation may also arise from heterogeneous and multi-phase reactions in both the organic and aqueous phases (Jimenez et al., 2009; Volkamer et al.,

65   2009). In turn, oxidant concentrations depend on shortwave fluxes (Tang et al., 1998; Tie, 2003; Yang et al., 2009). Smoke particles contain semivolatile organic compounds (SVOCs) (Eatough et al., 2003); (May et al., 2013), which may evaporate off of particles as the plume becomes more dilute (Formenti et al., 2003; Huffman et al., 2009; May et al., 2013), leading to losses in total aerosol mass. Field observations of smoke PM and OA mass normalized for dilution (e.g. through an inert tracer such as CO) report that for near-field (<24 hours) physical aging, net PM or OA mass can increase (Cachier et al.,

70   1995; Formenti et al., 2003; Liu et al., 2016; Nance et al., 1993; Reid et al., 1998; Vakkari et al., 2014, 2018; Yokelson et al., 2009), decrease (Akagi et al., 2012; Hobbs et al., 2003; Jolleys et al., 2012, 2015; May et al., 2015), or remain nearly

constant (Brito et al., 2014; Capes et al., 2008; Collier et al., 2016; Cubison et al., 2011; Forrister et al., 2015; Garofalo et al., 2019; Hecobian et al., 2011; Liu et al., 2016; May et al., 2015; Morgan et al., 2019; Sakamoto et al., 2015; Sedlacek et al., 2018; Zhou et al., 2017). It is theorized that both losses and gains in OA mass are likely happening concurrently in most

75 plumes through condensation and evaporation (Bian et al., 2017; Hodshire et al., 2019a, 2019b; May et al., 2015), with the balance between the two determining whether net increases or decreases or no change in mass occurs during near-field aging. However, there is currently no reliable predictor of how smoke aerosol mass (normalized for dilution) may change for a given fire.

Evolution of total aerosol number, size, and composition is critical in improving quantitative understanding of how

80 biomass burn smoke plumes impact climate. These impacts include smoke aerosols' abilities to both act as cloud condensation nuclei (CCN) and to scatter/absorb solar radiation, each of which is determined by particle size and composition (Albrecht, 1989; Petters and Kreidenweis, 2007; Seinfeld and Pandis, 2006; Twomey, 1974; Wang et al., 2008). Particles can increase or decrease in size as well as undergo compositional changes through condensation or evaporation of vapors. In contrast, coagulation always decreases total number concentrations and increases average particle diameter;

85 plumes with higher concentrations will undergo more coagulation than those with lower concentrations (Sakamoto et al., 2016).

Being able to predict smoke aerosol mass, number, size, and composition accurately is an essential component in constraining the influence of fires on climate, air quality, and health. Fires in the western United States region are predicted to increase in size, intensity, and frequency (Dennison et al., 2014; Ford et al., 2018; Spracklen et al., 2009; Yue et al.,

90 2013). In response, several large field campaigns have taken place in the last 7 years examining wildfires in this region (Kleinman and Sedlacek 2016; Garofalo et al. 2019). Here, we present smoke plume observations from the Biomass Burning Observation Project (BBOP) campaign of aerosol properties from five research flights sampling wildfires downwind in seven pseudo-Lagrangian sets of transects to investigate aging of OA mass and oxidation, and aerosol number and mean diameter. A range of initial plume OA mass concentrations were captured within these flights and sufficiently fast (1 second)

95 measurements of aerosols and key vapors were taken. We segregate each transect into edge, core, or intermediate regions of the plume and examine aerosol properties within the context of both the location within the plume (edge, core, or intermediate) and the initial OA mass loading of the given location, with the differences in aerosol loading serving as a proxy for differences in dilution rates, as the extent to which dilution has occurred prior to the first observation is not a measurable quantity. We create mathematical fits for predicting OA oxidation markers and mean particle diameter given

100 initial plume mass and physical age (time) of the smoke. These fits may be used to evaluate other smoke datasets and assist in building parameterizations for regional and global climate models to better-predict smoke aerosol climate and health impacts.

2 Methods

105   The BBOP field campaign occurred in 2013 and included a deployment of the United States Department of Energy
Gulfstream 1 (G-1) research aircraft in the Pacific Northwest region of the United States (Kleinman and Sedlacek, 2016;
Sedlacek et al., 2018) from June 15 to September 13. We analyze five cloud-free BBOP research flights that had seven total
sets of across-plume transects that followed the smoke plume downwind in a pseudo-Lagrangian manner (see Figs. S1-S6
for examples; Table S1) from approximately 15 minutes after emission to 2-4 hours downwind (Kleinman and Sedlacek,
2016). The G-1 sampling setup is described in (Kleinman and Sedlacek, 2016; Sedlacek et al., 2018; Kleinman et al., 2020).

110   Number size distributions were obtained with a Fast-integrating Mobility Spectrometer (FIMS), providing particle
size distributions nominally from ~20-350 nm (Kulkarni and Wang, 2006; Olfert and Wang, 2009); data was available
between 20-262 nm for the flights used in this study. A Soot Photometer Aerosol Mass Spectrometer (SP-AMS) provided
organic and inorganic (sulfate, chlorine, nitrate, ammonium) aerosol masses, select fractional components (the fraction of the
AMS OA spectra at a given mass-to-charge ratio) (Onasch et al., 2012), and elemental analysis (O/C and H/C) (Aiken et al.,

115   2008; Canagaratna et al., 2015). We use the f_{60} and f_{44} fractional components (the mass concentrations of m/z 60 and 44
normalized by the total OA mass concentration) and O/C and H/C elemental ratios of OA as tracers of smoke and oxidative
aging. Elevated f_{60} values are indicative of "levoglucosan-like" species (levoglucosan and other molecules that similarly
fragment in the AMS) (Aiken et al., 2009; Cubison et al., 2011; Lee et al., 2010) and are shown to be tracers of smoke
primary organic aerosol (POA) (Cubison et al., 2011). The f_{44} fractional component (arising from primarily CO_2+ as well as

120   some acid groups;) is indicative of SOA arising from oxidative aging (Alfarra et al., 2004; Cappa and Jimenez, 2010;
Jimenez et al., 2009; Volkamer et al., 2006). Fractional components f_{60} and f_{44} have been shown to decrease and increase
with photochemical aging, respectively, likely due to both evaporation and/or oxidation of semivolatile f_{60}-containing species
and addition of oxidized f_{44}-containing species (Alfarra et al., 2004; Huffman et al., 2009). O/C tends to increase with
oxidative aging (Decarlo et al., 2008) whereas H/C ranges from increasing to decreasing with oxidative aging, depending on

125   the types of reactions occurring (Heald et al., 2010). Thus, tracking H/C with aging may provide clues upon the types of
reactions that may be occuring. A Single-Particle Soot Photometer (SP2; Droplet Measurement Technologies) was used to
measure refractory black carbon (rBC) through laser-induced incandescence (Moteki and Kondo, 2010; Schwarz et al.,
2006). An Off-Axis Integrated-Cavity Output Spectroscopy instrument (Los Gatos, Model 907) provided CO measurements.
An SPN1 radiometer (Badosa et al., 2014; Long et al., 2010) provided total shortwave irradiance. The supporting

130   information includes more details on the instruments used.

To determine the contribution of species X from smoke, the background concentration of X is subtracted off and
normalized by background-corrected CO (ΔCO), which is inert on timescales of near-field aging (Yokelson et al., 2009), to
correct for dilution. Increases or decreases of ΔX/ΔCO with time indicate whether the total amount of X in the plume has
increased or decreased since time of emission. We background correct the number size distribution, OA, O, H, C, and rBC

135   data in this manner by determining an average regional background for each species by using the lowest 10% of the CO data

for a given flight with a similar altitude, latitude, and longitude as the smoke plume (excluding data from flying to and from the fire). Elemental O, H, and C are calculated using the O/C and H/C and OA data from the SP-AMS, allowing us to calculate $\Delta O/\Delta C$ and $\Delta H/\Delta C$. We also background-correct f_{60} and f_{44} (using the mass concentrations of m/z 60, m/z 44, and OA inside and outside of the plume), we but do not normalize by CO due to these values already being normalized by OA.

140 We only consider data to be in-plume if the absolute CO >= 150 ppbv, as comparisons of CO and the number concentration show that in-plume data has CO >150 ppbv and out-of-plume (background) data has CO < 150 ppbv. This threshold appears to be capturing clear plume features while excluding background air (Figs. S7-S11); we perform sensitivity analyses of our results to our assumptions about background and in-plume values in Section 3.

From the FIMS, we examine the background-corrected, normalized number concentrations of particles with

145 diameters between 40-262 nm, $\Delta N_{40-262\ nm}/\Delta CO$. $\Delta N_{40-262\ nm}/\Delta CO$ allows us to exclude potential influence of fresh nucleation upon the total number concentrations, as the bulk of observed newly formed particles observed fell below 40 nm (Figs. S7-S11). Smoke plumes contain particles with diameters larger than 262 nm (Janhäll et al., 2009), and so although we cannot provide total number concentrations, we can infer how the evolution of $\Delta N_{40-262\ nm}/\Delta CO$ will impact number concentrations overall. We also obtain an estimate of how the mean diameter between 40-262 nm, $\overline{D_p}$, changes with aging through:

150

$$\overline{D_p} = \frac{\Sigma N_i * D_{p,i}}{\Sigma N_i} \qquad\qquad \text{Eq. 1}$$

Where N_i and $D_{p,\ i}$ are the number concentration and geometric mean diameter within each FIMS size bin, respectively.

All of the data are provided at 1 Hz and all but the SP-AMS fractional component data are available on the DOE

155 ARM web archive (https://www.arm.gov /research/campaigns/aaf2013bbop). As the plane traveled at ~100 m s^{-1} on average, data were collected every 100 m across the plume. The instruments used here had a variety of time lags (all <10 seconds) relative to a TSI 3563 nephelometer used as reference. The FIMS also showed an additional lag in flushing smoky air with cleaner air when exiting the plume with maximum observed flushing timescales around 30 seconds, but generally less (Fig. S12). To test if these lags impact our results, we perform an additional analysis where we only consider the first half of each

160 in-plume transect, when concentrations are generally rising with time (Figure S12-S13), and our main conclusions are unaffected. We do not test the impacts of other timelags.

We use MODIS Terra and Aqua fire and thermal anomalies detection data to determine fire locations (Giglio et al., 2006, 2008) and estimate the fire center to be the approximate center of all clustered MODIS detection points for a given sampled fire (Figs. S1-S6). Depending upon the speed of the fire front, the true fire location and center at the time of

165 sampling is likely different than the MODIS estimates. To estimate the physical age of the plume, we use the estimated fire center as well as the FIMS number distribution to determine an approximate centerline of the plume as the smoke travels downwind (Figs. S1-S6) and use mean wind speed and this estimated centerline to get an estimated physical age for each

transect. We did not propagate uncertainty in fire location, wind speed, or centerline through to the physical age, which is a limitation of this study.

3 Results and discussion (as Heading 1)

As a case example, we examine the aging profiles of smoke from the Colockum fire during the first set of pseudo-Lagrangian transects on flight 730b (Table S1). Fig. 1 provides $\Delta OA/\Delta CO$, $\Delta rBC/\Delta CO$ Δf_{60}, Δf_{44}, $\Delta H/\Delta C$, $\Delta O/\Delta C$, $\Delta N_{40\text{-}262\ nm}/\Delta CO$, and $\overline{D_p}$ as a function of the estimated physical age; Figs. S14-S18 provide this information for the other pseudo-Lagrangian transect sets studied. We have divided each transect into four regions: between the 5-15 (edge), 15-50 (intermediate, outer), 50-90 (intermediate, inner), and 90-100 (core) percentile of ΔCO within each transect. Fig. 1 shows the edge and core data, both averaged per transect, with Figs. S14-18 providing all four percentile bins for each flight. These percentile bins correspond with the thinnest to thickest portions of the plume, respectively, and if a fire has uniform emissions ratios across all regions and dilutes evenly downwind, these percentile bins would correspond to the edges, intermediate regions, and the core of the diluting plume. We use this terminology in this study but note that uneven emissions, mixing, and/or dilution lead to the percentile bins not corresponding physically to our defined regions in some cases. However, the lowest two ΔCO bins tend more towards the physical edges of the plume and the highest two tend more towards the physical center of the plume (Figs. S2-S6). We do not use the data from the lowest 5% of ΔCO to reduce uncertainty at the plume-background boundary. We do not know where the plane is vertically in the plume, which is a limitation as vertical location will also impact the amount of solar flux able to penetrate through the plume.

Fig. 1 shows that $\Delta OA/\Delta CO$ and $\Delta rBC/\Delta CO$ vary little with age. A true Lagrangian flight with the aircraft sampling the same portion of the plume and no measurement artifacts (e.g. coincidence errors at high concentrations) would have a constant $\Delta rBC/\Delta CO$ for each transect. This flight and other flights studied here have slight variations in $\Delta rBC/\Delta CO$ (Fig. 1; Figs. S14-S18), which may be indicative of deviations from a Lagrangian flight path with temporal variations in emission and/or measurement uncertainties. For this flight, Δf_{60} changes little (~±6% between edge and core) while Δf_{44} increases slightly (~8% for both edge and core) with age, with edges showing the highest Δf_{44}. $\Delta H/\Delta C$ decreases while $\Delta O/\Delta C$ increases with the edges showing higher values of $\Delta O/\Delta C$. Mean aerosol diameter increases and normalized number concentration decreases between 40-262 nm with aging. The decrease in number concentration is presumably due to coagulation, as little dry deposition would occur within these timescales (<2.5 hours). These trends are discussed for all flights in the following sections.

3.1 Organic aerosol aging: $\Delta OA/\Delta CO$, Δf_{60}, Δf_{44}, $\Delta H/\Delta C$, and $\Delta O/\Delta C$

Fig. 2a-e show available $\Delta OA/\Delta CO$, Δf_{60}, Δf_{44} $\Delta H/\Delta C$, and $\Delta O/\Delta C$ edge and core data versus physical age for each transect for each flight of this study, colored by the mean ΔOA within a ΔCO percentile bin from the transect closest to

the fire, $\Delta OA_{initial}$. We show the 5-15 (edge) and 90-100 (core) ΔCO percentile bins here; Fig. S19 shows the same

200   information for all four ΔCO percentiles. We note that although some of the physical ages appear to be at ~0 hours, this is

from a limitation of our physical age estimation method (Sect. 2), as no flights captured data before ~15 minutes after

emission (Kleinman et al., 2016). Also included in Fig. 2 are the Spearman rank-order correlation tests (hereafter Spearman

tests) that show correlation coefficients (R) with initial plume OA mass, $\Delta OA_{initial}$ ($R_{\Delta OA,initial}$), and physical age (R_{age})

against each variable (for the correlations with $\Delta OA_{initial}$, all transects in a set are given the same $\Delta OA_{initial}$ value). Figs. S13,

205   S19-S21 show the same details as Fig. 2 but provide sensitivity tests to potential FIMS measurement artifacts (Fig. S13) and

our assumed background CO and ΔCO percentile spacing (Figs. S19-S21). Although these Figs. show slight variability, the

findings discussed below remain robust and we constrain the rest of our discussion to the FIMS measurements and

background and ΔCO percentile spacings used in Fig. 2.

In general, both the cores and edges show little change in $\Delta OA/\Delta CO$ with physical aging, with $R_{\Delta OA,initial}$ and R_{age}

210   both at 0.03 (the absolute variability is dominated by differences between plumes). While the observed trends in $\Delta OA/\Delta CO$

with aging are small, Δf_{60} and Δf_{44} show clear signs of changes with aging, consistent with previous studies(Cubison et al.,

2011; Garofalo et al., 2019; May et al., 2015). Spearman tests on physical age vs. Δf_{60} and Δf_{44} give R_{age} values of -0.25 and

0.54, respectively. Δf_{60} generally decreases with plume age, consistent with the hypotheses that Δf_{60} may be evaporating off

through heterogeneous oxidation and/or has a decreasing fractional contribution due to condensation of other compounds. In

215   contrast, Δf_{44} generally increases with age for all plumes with available data, and hence it would appear that for plumes with

little change in $\Delta OA/\Delta CO$, evaporation of f_{60}-containing compounds is roughly balanced by condensation of more-oxidized

compounds, including those that contain f_{44}, suggesting the possibility that heterogeneous or particle-phase oxidation that

would alter the balance of Δf_{60}, and Δf_{44}. However, estimates of heterogeneous mass losses indicate that after three hours of

aging for a range of OH concentrations and reactive uptake coefficients over 90% of aerosol mass remains (Fig. S23; see SI

220   text S2 for more details on the calculation).

Two more important features of Δf_{60} and Δf_{44} can be seen within Fig. 2: (1) Δf_{60} and Δf_{44} depend on $\Delta OA_{initial}$

($R_{\Delta OA,initial}$ = 0.38 and -0.5, respectively), with more concentrated plumes having consistently higher Δf_{60} and lower Δf_{44}. (2)

Differences in Δf_{60} and Δf_{44} for the nearest-to-source measurements indicate that evaporation and/or chemistry likely

occurred before the time of these first measurements (assuming that emitted Δf_{60} and Δf_{44} do not correlate with $\Delta OA_{initial}$).

225   The amounts of evaporation and/or chemistry depend on $\Delta OA_{initial}$, with higher rates of evaporation and chemistry occurring

for lower values of $\Delta OA_{initial}$. This result is consistent with the hypothesis that aircraft observations are missing evaporation

and chemistry prior to the first aircraft observation (Hodshire et al., 2019b). The differences in $\Delta OA_{initial}$ between plumes

may be due to different emissions fluxes (e.g., due to different fuels or combustion phases), or plume widths, where

larger/thicker plumes dilute more slowly than smaller/thinner plumes; these larger plumes have been predicted to have less

230   evaporation and may undergo relatively less photooxidation (Bian et al., 2017; Hodshire et al., 2019a, 2019b).

(Garofalo et al., 2019) segregated smoke data from the WE-CAN field campaign by distance from the center of a

given plume and showed that the edges of one of the fires studied have less f_{60} and more f_{44} (not background-corrected) than

the core of the plume. Similarly, we find that the 730b flight shows a very similar pattern in f_{60} and f_{44} (Figs. S24-S25) to that shown in (Garofalo et al., 2019) (their Fig. 6). The 821b and 809a flights also hint at elevated f_{44} and decreased f_{60} at the

235   edges but the remaining plumes do not show a clear trend from edge to core in f_{60} and f_{44}. This could be as CO concentrations (and thus presumably other species) do not evenly increase from the edge to the core for many of the plume transects studied (Figs. S2-S6). We do not have UV measurements that allow us to calculate photolysis rates but the in-plume shortwave measurements in the visible show a dimming in the fresh cores that has a similar pattern to f_{44} and the inverse of f_{60} (Fig. S26; the rapid oscillations in this figure could be indicative of sporadic cloud cover above the plumes).

240   We also plot core and edge $\Delta H/\Delta C$ and $\Delta O/\Delta C$ as a function of physical age (Fig. 2d-e). Similar to Δf_{44}, $\Delta O/\Delta C$ increases with physical age and is well correlated to both physical age and $\Delta OA_{initial}$ (R_{age} = 0.61 and $R_{\Delta OA,initial}$ = -0.42). Conversely, $\Delta H/\Delta C$ tends to be fairly constant or slightly decreasing with physical age and is poorly correlated to physical age and $\Delta OA_{initial}$. A Van Krevelen diagram of $\Delta H/\Delta C$ versus $\Delta O/\Delta C$ (Fig. S27) indicates that oxygenation reactions or a combination of oxygenation and hydration reactions are likely dominant (Heald et al., 2010); however, without further

245   information, we cannot conclude which reactions are occurring.

Both physical age and $\Delta OA_{initial}$ appear to influence Δf_{60}, Δf_{44}, and $\Delta O/\Delta C$: oxidation reactions and evaporation from dilution occur with aging, and the extent of photochemistry and dilution should depend on plume thickness. Being able to predict biomass burning aerosol aging parameters can provide a framework for interstudy-comparisons and can aid in modeling efforts. We construct mathematical fits for predicting Δf_{60}, Δf_{44}, and $\Delta O/\Delta C$:

250

$$X = a \, log_{10}(\Delta OA_{initial}) + b \, (Physical \, age) \, + c \qquad\qquad \text{Eq. 2}$$

where X is Δf_{60}, Δf_{44}, or $\Delta O/\Delta C$ and a, b, and c are fit coefficients. The measured vs. fit data and values of a, b, and c are shown in Fig. 3a-c. The Pearson and Spearman coefficients of determination (R^2_p and R^2_s, respectively) are also summarized

255   in Fig. 3 and indicate moderate goodness of fits (R^2 between 0.21-0.25 for Δf_{60}, between 0.53-0.58 for Δf_{44}, and between 0.41-0.58 for $\Delta O/\Delta C$). Although no models that we are aware of currently predict aerosol fractional components (e.g. f_{60} or f_{44}), O/H and H/C are predicted by some models (e.g., (Cappa and Wilson, 2012) and these fit parameters may assist in biomass burning modeling.

Other functional fits were explored (Figs. S28-S29), with

260

$$ln(\Delta X) = a \, ln(\Delta OA_{initial}) + b \, ln(Physical \, age) \, + c \qquad\qquad \text{Eq. 3}$$

(Fig. S28) and $\Delta N_{initial}$ in the place of $\Delta OA_{initial}$ in Eq. 2 (Fig. S29) providing similar fits for Δf_{60} and Δf_{44}. Aged Δf_{60} and Δf_{44} show scatter, limiting the predictive skill of measurements available from BBOP. The scatter is likely to variability in

265   emissions due to source fuel or combustion conditions, instrument noise and response under large concentration ranges encountered in these smoke plumes, inhomogeneous mixing within the plume, variability in background concentrations not

Atmospheric
Chemistry
and Physics
Discussions

captured by our background correction method, inaccurate characterizations of physical age due to variable wind speed, and deviations from a true Lagrangian flight path. There may be another variable not available to us from the BBOP data that aids this prediction, such as photolysis rates. We encourage these fits to be tested out with further data sets and modeling.

270 **3.2 Aerosol size distribution properties: $\Delta N_{40-262\ nm}/\Delta CO$ and $\overline{D_p}$**

The observations of the normalized number concentration between 40-262 nm, $\Delta N_{40-262\ nm}/\Delta CO$ (Fig. 2f), show that plume edges and cores generally show decreases in $\Delta N_{40-262\ nm}/\Delta CO$ with physical age, with R_{age} = -0.25. The plume edges and cores with the highest initial ΔOA generally have lower normalized number concentrations by the time of the first measurement, and the edges generally have higher initial normalized number concentrations than the cores, potentially due

275 to differences in coagulation rates. A few dense cores have normalized number concentrations comparable or higher than the thinner edges, leading to no correlation with $\Delta OA_{initial}$. We note that variability in number emissions (due to e.g. burn conditions) adds noise not captured by the R values.

The mean particle size between 40-262 nm, $\overline{D_p}$ (Eq. 1), is shown to increase with aging (Fig. 2g) for all plumes (R_{age} = 0.48). Coagulation and SOA condensation will increase $\overline{D_p}$ and OA evaporation will decrease $\overline{D_p}$. The plumes do not

280 show significant changes in $\Delta OA/\Delta CO$ (Fig. 2a), indicating that coagulation is likely responsible for the majority of increases in $\overline{D_p}$. The functional fits for Δf_{60} and Δf_{44} (Eq. 2; where X is $\overline{D_p}$ in this case) can also moderately predict $\overline{D_p}$ (R^2_p and R^2_s of 0.36 and 0.31; Fig. 3d) but do not well-predict $\Delta N_{40-300\ nm}/\Delta CO$ (not shown). Sakamoto et al. (2016) provide fit equations for modeled $\overline{D_p}$ as a function of age, but they include a known initial $\overline{D_p}$ at the time of emission in their parameterization, which is not available here. $\Delta N_{initial}$ in the place of $\Delta OA_{initial}$ in Eq. 2 predicts $\overline{D_p}$ similarly (Fig. S29). As

285 discussed in Section 3.1, scatter in number concentrations limits our prediction skill.

Nucleation-mode particles (inferred in this study from particles appearing between 20-40 nm in the FIMS measurements) are observed for some of the transects (S7-S11). Some days also show nucleation-mode particles downwind of fires in between transects (Figs. S7, S8, S9, and S11). Nucleation-mode particles appear to primarily occur in the outer portion of plumes, although one day did show nucleation-mode particles within the core of the plume (Fig. S11). Nucleation

290 at edges could be due to increased photooxidation from higher total irradiance relative to the core (Fig. S26). However, given the relatively small number of data points showing nucleation mode particles and limited photooxidation and gas-phase information, we do not have confidence in the underlying source of the nucleation-mode particles. The nucleation mode tends to be ~one order of magnitude less concentrated than the larger particles, and appears to be coagulating or evaporating away as the plumes travel downwind.

Atmospheric
Chemistry
and Physics
Discussions

4 Summary and outlook

The BBOP field campaign provided high time resolution (1 s) measurements of gas- and particle-phase smoke measurements downwind of western U.S. wildfires along pseudo-Lagrangian transects. These flights have allowed us to examine near-field (<4 hours) aging of smoke particles to provide analyses on how these species vary across a range of initial aerosol mass loadings (a proxy for the relative rates at which the plume is anticipated to dilute as dilution before the first observation is not a measurable quantity) as well as how they vary between the edges and cores of each plume. We find that although $\Delta OA/\Delta CO$ shows little variability, Δf_{60} (a marker for evaporation) decreases with physical aging; Δf_{44} and $\Delta O/\Delta C$ (markers for photochemical aging) increases with physical aging; and each correlate with both $\Delta OA_{initial}$ and physical age. $\Delta N_{40\text{-}262\ nm}/\Delta CO$ decreases with physical aging through coagulation, with thicker plumes tending to show lower number concentrations, indicative of higher rates of coagulation. Mean aerosol diameter between 40-262 nm increases with age primarily due to coagulation, as organic aerosol mass does not change significantly. Nucleation is observed within a few of the fires and appears to occur primarily on the edges of the plumes. Differences in initial values of Δf_{60}, Δf_{44}, and $\Delta O/\Delta C$ between higher- and lower-concentrated plumes indicate that evaporation and/or chemistry has likely occurred before the time of initial measurement and that plumes or plume regions (such as the outer parts of the plume) with lower initial aerosol loading can undergo these changes more rapidly than thicker plumes. We encourage future studies to attempt to quantify these chemical and physical changes before the initial measurement using combinations of modeling and laboratory measurements, where sampling is possible at the initial stages of the fire and smoke. We also encourage future near-field (<24 hours) analyses of recent and future biomass burning field campaigns to include differences in initial plume mass concentrations and location within the plume as considerations for understanding chemical and physical processes in plumes.

Atmospheric
Chemistry
and Physics
Discussions

References

Adachi, K., Sedlacek, A. J., Kleinman, L., Springston, S. R., Wang, J. and Chand, D.: Spherical tarball particles form
      through rapid chemical and physical changes of organic matter in biomass-burning smoke, Proceedings of the
      National Academy of Sciences, 1–6, 2019.

Aiken, A. C., Decarlo, P. F., Kroll, J. H., Worsnop, D. R., Huffman, J. A., Docherty, K. S., Ulbrich, I. M., Mohr, C.,
335   Kimmel, J. R., Sueper, D., Sun, Y., Zhang, Q., Trimborn, A., Northway, M., Ziemann, P. J., Canagaratna, M. R.,
      Onasch, T. B., Alfarra, M. R., Prevot, A. S. H., Dommen, J., Duplissy, J., Metzger, A., Baltensperger, U. and
      Jimenez, J. L.: O/C and OM/OC ratios of primary, secondary, and ambient organic aerosols with high-resolution
      time-of-flight aerosol mass spectrometry, Environmental Science and Technology, 42(12), 4478–4485, 2008.

Aiken, A. C., Salcedo, D., Cubison, M. J., Huffman, J. A., DeCarlo, P. F., Ulbrich, I. M., Docherty, K. S., Sueper, D.,
340   Kimmel, J. R., Worsnop, D. R. and Others: Mexico City aerosol analysis during MILAGRO using high resolution
      aerosol mass spectrometry at the urban supersite (T0)--Part 1: Fine particle composition and organic source
      apportionment, Atmos. Chem. Phys., 9(17), 6633–6653, 2009.

Akagi, S. K., Yokelson, R. J., Wiedinmyer, C., Alvarado, M. J., Reid, J. S., Karl, T., Crounse, J. D. and Wennberg, P. O.:
      Emission factors for open and domestic biomass burning for use in atmospheric models, Atmos. Chem. Phys.,
345   11(9), 4039–4072, 2011.

Akagi, S. K., Craven, J. S., Taylor, J. W., Mcmeeking, G. R., Yokelson, R. J., Burling, I. R., Urbanski, S. P., Wold, C. E.,
      Seinfeld, J. H., Coe, H., Alvarado, M. J. and Weise, D. R.: Evolution of trace gases and particles emitted by a
      chaparral fire in California, Atmos. Chem. Phys., 12, 1397–1421, 2012.

Albrecht, B. A.: Aerosols, cloud microphysics, and fractional cloudiness, Science, 245(4923), 1227–1230, 1989.

350   Alfarra, M. R., Coe, H., Allan, J. D., Bower, K. N., Boudries, H., Canagaratna, M. R., Jimenez, J. L., Jayne, J. T., Garforth,
      A. A., Li, S.-M. and Worsnop, D. R.: Characterization of urban and rural organic particulate in the Lower Fraser
      Valley using two Aerodyne Aerosol Mass Spectrometers, Atmos. Environ., 38(34), 5745–5758, 2004.

Andela, N., Morton, D. C., Giglio, L., Paugam, R., Chen, Y., Hantson, S., Werf, G. R. and Randerson, J. T.: The Global Fire
      Atlas of individual fire size, duration, speed and direction, Earth System Science Data, 11(2), 529–552, 2019.

355 Badosa, J., Wood, J., Blanc, P., Long, C. N., Vuilleumier, L., Demengel, D. and Haeffelin, M.: Solar irradiances measured
       using SPN1 radiometers: uncertainties and clues for development, Atmospheric Measurement Techniques, 7, 4267–
       4283, 2014.

Bian, Q., Jathar, S. H., Kodros, J. K., Barsanti, K. C., Hatch, L. E., May, A. A., Kreidenweis, S. M. and Pierce, J. R.:
       Secondary organic aerosol formation in biomass-burning plumes: Theoretical analysis of lab studies and ambient
360   plumes, Atmos. Chem. Phys., 17(8), 5459–5475, 2017.

Brito, J., Rizzo, L. V., Morgan, W. T., Coe, H., Johnson, B., Haywood, J., Longo, K., Freitas, S., Andreae, M. O. and
       Artaxo, P.: Ground-based aerosol characterization during the South American Biomass Burning Analysis
       (SAMBBA) field experiment, Atmospheric Chemistry and Physics, 14(22), 12069–12083, doi:10.5194/acp-14-
       12069-2014, 2014.

365 Cachier, H., Liousse, C., Buat-Menard, P. and Gaudichet, A.: Particulate content of savanna fire emissions, J. Atmos. Chem.,
       22(1-2), 123–148, 1995.

Canagaratna, M. R., Jimenez, J. L., Kroll, J. H., Chen, Q., Kessler, S. H., Massoli, P., Hildebrandt Ruiz, L., Fortner, E.,
       Williams, L. R., Wilson, K. R. and Others: Elemental ration measurements of organic compounds using aerosol
       mass spectrometry: characterization, improved calibration, and implications, Atmos. Chem. Phys., 15, 253–272,
370   2015.

Capes, G., Johnson, B., McFiggans, G., Williams, P. I., Haywood, J. and Coe, H.: Aging of biomass burning aerosols over
       West Africa: Aircraft measurements of chemical composition, microphysical properties, and emission ratios, J.
       Geophys. Res. D: Atmos., 113(23), 0–15, 2008.

Cappa, C. D. and Jimenez, J. L.: Quantitative estimates of the volatility of ambient organic aerosol, Atmos. Chem. Phys.,
375   10(12), 5409–5424, 2010.

Cappa, C. D. and Wilson, K. R.: Multi-generation gas-phase oxidation, equilibrium partitioning, and the formation and
       evolution of secondary organic aerosol, Atmos. Chem. Phys., 12(20), 9505–9528, 2012.

Carrico, C. M., Petters, M. D., Kreidenweis, S. M., Collett, J. L., Jr., Engling, G. and Malm, W. C.: Aerosol hygroscopicity
       and cloud droplet activation of extracts of filters from biomass burning experiments, J. Geophys. Res., 113(D8),
380   4767, 2008.

Collier, S., Zhou, S., Onasch, T. B., Jaffe, D. A., Kleinman, L., Sedlacek, A. J., Briggs, N. L., Hee, J., Fortner, E., Shilling, J.
       E., Worsnop, D., Yokelson, R. J., Parworth, C., Ge, X., Xu, J., Butterfield, Z., Chand, D., Dubey, M. K., Pekour, M.
       S., Springston, S. and Zhang, Q.: Regional Influence of Aerosol Emissions from Wildfires Driven by Combustion
       Efficiency: Insights from the BBOP Campaign, Environmental Science and Technology, 50(16), 8613–8622, 2016.

385 Cubison, M. J., Ortega, A. M., Hayes, P. L., Farmer, D. K., Day, D., Lechner, M. J., Brune, W. H., Apel, E., Diskin, G. S.,
       Fisher, J. A., Fuelberg, H. E., Hecobian, A., Knapp, D. J., Mikoviny, T., Riemer, D., Sachse, G. W., Sessions, W.,
       Weber, R. J., Weinheimer, A. J., Wisthaler, A. and Jimenez, J. L.: Effects of aging on organic aerosol from open
       biomass burning smoke in aircraft and laboratory studies, Atmos. Chem. Phys., 11(23), 12049–12064, 2011.

390   Decarlo, P. F., Dunlea, E. J., Kimmel, J. R., Aiken, A. C., Sueper, D., Crounse, J., Wennberg, P. O., Emmons, L., Shinozuka, Y., Clarke, A., Zhou, J., Tomlinson, J., Collins, D. R., Knapp, D., Weinheimer, A. J., Montzka, D. D., Campos, T. and Jimenez, J. L.: Fast airborne aerosol size and chemistry measurements above Mexico City and Central Mexico during the MILAGRO campaign., 2008.

Dennison, P. E., Brewer, S. C., Arnold, J. D. and Moritz, M. A.: Large wildfire trends in the western United States, 1984-2011, Geophysical Research Letters, 41(8), 2928–2933, doi:10.1002/2014gl059576, 2014.

395   Eatough, D. J., Eatough, N. L., Pang, Y., Sizemore, S., Kirchstetter, T. W., Novakov, T. and Hobbs, P. V.: Semivolatile particulate organic material in southern Africa during SAFARI 2000, J. Geophys. Res. D: Atmos., 108(D13) [online] Available from: https://agupubs.onlinelibrary.wiley.com/doi/abs/10.1029/2002JD002296%4010.1002/%28ISSN%292169-8996.SAF1, 2003.

400   Ford, B., Val Martin, M., Zelasky, S. E., Fischer, E. V., Anenberg, S. C., Heald, C. L. and Pierce, J. R.: Future Fire Impacts on Smoke Concentrations, Visibility, and Health in the Contiguous United States, GeoHealth, doi:10.1029/2018GH000144, 2018.

Formenti, P., Elbert, W., Maenhaut, W., Haywood, J., Osborne, S. and Andreae, M. O.: Inorganic and carbonaceous aerosols during the Southern African Regional Science Initiative (SAFARI 2000) experiment: Chemical characteristics, physical properties, and emission data for smoke from African biomass burning, J. Geophys. Res. D: Atmos., 108(D13), doi:10.1029/2002JD002408, 2003.

Forrister, H., Liu, J., Scheuer, E., Dibb, J., Ziemba, L., Thornhill, K. L., Anderson, B., Diskin, G., Perring, A. E., Schwarz, J. P., Campuzano-Jost, P., Day, D. A., Palm, B. B., Jimenez, J. L., Nenes, A. and Weber, R. J.: Evolution of brown carbon in wildfire plumes, Geophys. Res. Lett., 42(11), 4623–4630, 2015.

410   Gan, R. W., Ford, B., Lassman, W., Pfister, G., Vaidyanathan, A., Fischer, E., Volckens, J., Pierce, J. R. and Magzamen, S.: Comparison of wildfire smoke estimation methods and associations with cardiopulmonary-related hospital admissions, GeoHealth, 1(3), 122–136, 2017.

Garofalo, L., Pothier, M. A., Levin, E. J. T., Campos, T., Kreidenweis, S. M. and Farmer, D. K.: Emission and Evolution of Submicron Organic Aerosol in Smoke from Wildfires in the Western United States, ACS Earth and Space Chemistry, acsearthspacechem.9b00125, 2019.

Giglio, L., Csiszar, I. and Justice, C. O.: Global distribution and seasonality of active fires as observed with the Terra and Aqua Moderate Resolution Imaging Spectroradiometer (MODIS) sensors, Journal of Geophysical Research: Biogeosciences, 111(G2) [online] Available from: https://agupubs.onlinelibrary.wiley.com/doi/abs/10.1029/2005JG000142, 2006.

420   Giglio, L., Csiszar, I., Restás, Á., Morisette, J. T., Schroeder, W., Morton, D. and Justice, C. O.: Active fire detection and characterization with the advanced spaceborne thermal emission and reflection radiometer (ASTER), Remote Sensing of Environment, 112(6), 3055–3063, doi:10.1016/j.rse.2008.03.003, 2008.

Gilman, J. B., Lerner, B. M., Kuster, W. C., Goldan, P. D., Warneke, C., Veres, P. R., Roberts, J. M., De Gouw, J. A.,
Burling, I. R. and Yokelson, R. J.: Biomass burning emissions and potential air quality impacts of volatile organic
425   compounds and other trace gases from fuels common in the US, Atmos. Chem. Phys., 15(24), 13915–13938, 2015.

Hatch, L. E., Luo, W., Pankow, J. F., Yokelson, R. J., Stockwell, C. E. and Barsanti, K. C.: Identification and quantification
of gaseous organic compounds emitted from biomass burning using two-dimensional gas chromatography-time-of-
flight mass spectrometry, Atmos. Chem. Phys., 15(4), 1865–1899, 2015.

Hatch, L. E., Yokelson, R. J., Stockwell, C. E., Veres, P. R., Simpson, I. J., Blake, D. R., Orlando, J. J. and Barsanti, K. C.:
430   Multi-instrument comparison and compilation of non-methane organic gas emissions from biomass burning and
implications for smoke-derived secondary organic aerosol precursors, Atmos. Chem. Phys., 17, 1471–1489, 2017.

Heald, C. L., Kroll, J. H., Jimenez, J. L., Docherty, K. S., DeCarlo, P. F., Aiken, A. C., Chen, Q., Martin, S. T., Farmer, D.
K. and Artaxo, P.: A simplified description of the evolution of organic aerosol composition in the atmosphere,
Geophys. Res. Lett., 37(8), doi:10.1029/2010GL042737, 2010.

435   Hecobian, A., Liu, Z., Hennigan, C. J., Huey, L. G., Jimenez, J. L., Cubison, M. J., Vay, S., Diskin, G. S., Sachse, G. W.,
Wisthaler, A., Mikoviny, T., Weinheimer, A. J., Liao, J., Knapp, D. J., Wennberg, P. O., Urten, A., Crounse, J. D.,
Clair, J. S., Wang, Y. and Weber, R. J.: Comparison of chemical characteristics of 495 biomass burning plumes
intercepted by the NASA DC-8 aircraft during the ARCTAS/CARB-2008 field campaign, Atmos. Chem. Phys., 11,
13325–13337, 2011.

440   Hobbs, P. V., Sinha, P., Yokelson, R. J., Christian, T. J., Blake, D. R., Gao, S., Kirchstetter, T. W., Novakov, T. and
Pilewskie, P.: Evolution of gases and particles from a savanna fire in South Africa, J. Geophys. Res. D: Atmos.,
108(D13), doi:10.1029/2002JD002352, 2003.

Hodshire, A. L., Akherati, A., Alvarado, M. J., Brown-Steiner, B., Jathar, S. H., Jimenez, J. L., Kreidenweis, S. M.,
Lonsdale, C. R., Onasch, T. B., Ortega, A. M. and Pierce, J. R.: Aging Effects on Biomass Burning Aerosol Mass
445   and Composition: A Critical Review of Field and Laboratory Studies, Environ. Sci. Technol., 53(17), 10007–
10022, 2019a.

Hodshire, A. L., Bian, Q., Ramnarine, E., Lonsdale, C. R., Alvarado, M. J., Kreidenweis, S. M., Jathar, S. H. and Pierce, J.
R.: More than emissions and chemistry: Fire size, dilution, and background aerosol also greatly influence near-field
biomass burning aerosol aging, J. Geophys. Res. D: Atmos., 2018JD029674, 2019b.

450   Huffman, J. A., Docherty, K. S., Aiken, A. C., Cubison, M. J., Ulbrich, I. M., Decarlo, P. F., Sueper, D., Jayne, J. T.,
Worsnop, D. R., Ziemann, P. J. and Jimenez, J. L.: Chemically-resolved aerosol volatility measurements from two
megacity field studies., 2009.

Janhäll, S., Andreae, M. O. and Pöschl, U.: Biomass burning aerosol emissions from vegetation fires: particle number and
mass emission factors and size distributions, Atmos. Chem. Phys. Disc., 9(4), 17183–17217, 2009.

Atmospheric
Chemistry
and Physics
Discussions
Open Access
EGU

455 Jen, C. N., Hatch, L. E., Selimovic, V., Yokelson, R. J., Weber, R., Fernandez, A. E., Kreisberg, N. M., Barsanti, K. C. and
        Goldstein, A. H.: Speciated and total emission factors of particulate organics from burning western US wildland
        fuels and their dependence on combustion efficiency, Atmos. Chem. Phys., 19, 1013–1026, 2019.

Jimenez, J. L., Canagaratna, M. R., Donahue, N. M., Prevot, a. S. H., Zhang, Q., Kroll, J. H., DeCarlo, P. F., Allan, J. D.,
        Coe, H., Ng, N. L., Aiken, a. C., Docherty, K. S., Ulbrich, I. M., Grieshop, a. P., Robinson, a. L., Duplissy, J.,
460   Smith, J. D., Wilson, K. R., Lanz, V. a., Hueglin, C., Sun, Y. L., Tian, J., Laaksonen, A., Raatikainen, T.,
        Rautiainen, J., Vaattovaara, P., Ehn, M., Kulmala, M., Tomlinson, J. M., Collins, D. R., Cubison, M. J., Dunlea, E.
        J., Huffman, J. a., Onasch, T. B., Alfarra, M. R., Williams, P. I., Bower, K., Kondo, Y., Schneider, J., Drewnick, F.,
        Borrmann, S., Weimer, S., Demerjian, K., Salcedo, D., Cottrell, L., Griffin, R., Takami, A., Miyoshi, T.,
        Hatakeyama, S., Shimono, A., Sun, J. Y., Zhang, Y. M., Dzepina, K., Kimmel, J. R., Sueper, D., Jayne, J. T.,
465   Herndon, S. C., Trimborn, a. M., Williams, L. R., Wood, E. C., Middlebrook, a. M., Kolb, C. E., Baltensperger, U.
        and Worsnop, D. R.: Evolution of organic aerosols in the atmosphere, Science, 326(5959), 1525–1529, 2009.

Jolleys, M. D., Coe, H., McFiggans, G., Capes, G., Allan, J. D., Crosier, J., Williams, P. I., Allen, G., Bower, K. N., Jimenez,
        J. L., Russell, L. M., Grutter, M. and Baumgardner, D.: Characterizing the aging of biomass burning organic aerosol
        by use of mixing ratios: A meta-analysis of four regions, Environmental Science and Technology, 46(24), 13093–
470   13102, 2012.

Jolleys, M. D., Coe, H., McFiggans, G., Taylor, J. W., O'Shea, S. J., Le Breton, M., Bauguitte, S. J. B., Moller, S., Di Carlo,
        P., Aruffo, E., Palmer, P. I., Lee, J. D., Percival, C. J. and Gallagher, M. W.: Properties and evolution of biomass
        burning organic aerosol from Canadian boreal forest fires, Atmos. Chem. Phys., 15(6), 3077–3095, 2015.

Kleinman, L. and Sedlacek, A. J., III: Biomass Burning Observation Project (BBOP) Final Campaign Report, 2016.

475 Kleinman, L. I., Sedlacek, A. J., III, Adachi, K., Buseck, P. R., Collier, S., Dubey, M., K., Hodshire, A. L., Lewis, E.,
        Onasch, T. B., Pierce, J. R., Schilling, J., Springston, S. R., Wang, J., Zhang, Q., Zhoui, S., Yokelson, R. J.: Rapid
        Evolution of Aerosol Particles and their Optical Properties Downwind of Wildfires in the Western U.S., submitted
        to Atmos. Chem. Phys., 2020.

Konovalov, I. B., Beekmann, M., Golovushkin, N. A. and Andreae, M. O.: Nonlinear behavior of organic aerosol in biomass
480   burning plumes: a microphysical model analysis, Atmos. Chem. Phys. Disc., 1–44, 2019.

Koss, A. R., Sekimoto, K., Gilman, J. B., Selimovic, V., Coggon, M. M., Zarzana, K. J., Yuan, B., Lerner, B. M., Brown, S.
        S., Jimenez, J. L., Krechmer, J., Roberts, J. M., Warneke, C., Yokelson, R. J. and De Gouw, J.: Non-methane
        organic gas emissions from biomass burning: Identification, quantification, and emission factors from PTR-ToF
        during the FIREX 2016 laboratory experiment, Atmos. Chem. Phys., 18(5), 3299–3319, 2018.

485 Kroll, J. H. and Seinfeld, J. H.: Chemistry of secondary organic aerosol: Formation and evolution of low-volatility organics
        in the atmosphere, Atmos. Environ., 42, 3593–3624, 2008.

Kulkarni, P. and Wang, J.: New fast integrated mobility spectrometer for real-time measurement of aerosol size
        distribution—I: Concept and theory, J. Aerosol Sci., 37(10), 1303–1325, 2006.

Atmospheric
Chemistry
and Physics
Discussions

Lee, T., Sullivan, A. P., Mack, L., Jimenez, J. L., Kreidenweis, S. M., Onasch, T. B., Worsnop, D. R., Malm, W., Wold, C.
490   E., Hao, W. M. and Collett, J. L.: Chemical Smoke Marker Emissions During Flaming and Smoldering Phases of
Laboratory Open Burning of Wildland Fuels, Aerosol Sci. Technol., 44(9), i–v, 2010.

Liu, X., Zhang, Y., Huey, L. G., Yokelson, R. J., Wang, Y., Jimenez, J. L., Campuzano-Jost, P., Beyersdorf, A. J., Blake, D.
R., Choi, Y., St. Clair, J. M., Crounse, J. D., Day, D. A., Diskin, G. S., Ried, A., Hall, S. R., Hanisco, T. F., King, L.
495   E., Meinardi, S., Mikoviny, T., Palm, B. B., Peischl, J., Perring, A. E., Pollack, I. B., Ryerson, T. B., Sachse, G.,
Schwarz, J. P., Simpson, I. J., Tanner, D. J., Thornhil, K. L., Ullmann, K., Weber, R. J., Wennberg, P. O.,
Wisthaler, A., Wolfe, G. M. and Ziemba, L. D.: Agricultural fires in the southeastern U.S. during SEAC4RS:
Emissions of trace gases and particles and evolution of ozone, reactive nitrogen, and organic aerosol, J. Geophys.
Res., 121(12), 7383–7414, 2016.

Long, C. N., Bucholtz, A., Jonsson, H., Schmid, B., Vogelmann, A. and Wood, J.: A Method of Correcting for Tilt from
500   Horizontal in Downwelling Shortwave Irradiance Measurements on Moving Platforms, The Open Atmospheric
Science Journal, 4(1), 78–87, doi:10.2174/1874282301004010078, 2010.

May, A. A., Levin, E. J. T., Hennigan, C. J., Riipinen, I., Lee, T., Collett, J. L., Jimenez, J. L., Kreidenweis, S. M. and
Robinson, A. L.: Gas-particle partitioning of primary organic aerosol emissions: 3. Biomass burning, J. Geophys.
Res. D: Atmos., 118(19), 11327–11338, 2013.

505   May, A. A., Lee, T., McMeeking, G. R., Akagi, S., Sullivan, A. P., Urbanski, S., Yokelson, R. J. and Kreidenweis, S. M.:
Observations and analysis of organic aerosol evolution in some prescribed fire smoke plumes, Atmos. Chem. Phys.,
15(11), 6323–6335, 2015.

Morgan, W. T., Allan, J. D., Bauguitte, S., Darbyshire, E., Flynn, M. J., Lee, J., Liu, D., Johnson, B., Haywood, J., Longo,
K. M., Artaxo, P. E. and Coe, H.: Transformation and aging of biomass burning carbonaceous aerosol over tropical
510   South America from aircraft in-situ measurements during SAMBBA, Atmos. Chem. Phys. Discuss.,
doi:10.5194/acp-2019-157, 2019.

Moteki, N. and Kondo, Y.: Dependence of Laser-Induced Incandescence on Physical Properties of Black Carbon Aerosols:
Measurements and Theoretical Interpretation, Aerosol Sci. Technol., 44(8), 663–675, 2010.

Nance, J. D., Hobbs, P. V. and Radkel, L. F.: Airborne Measurements of Gases and Particles From an Alaskan Wildfire, J.
515   Geophys. Res. D: Atmos., 98(D8), 873–882, 1993.

Noyes, K. J., Kahn, R., Sedlacek, A., Kleinman, L., Limbacher, J. and Li, Z.: Wildfire Smoke Particle Properties and
Evolution, from Space-Based Multi-Angle Imaging, Remote Sensing, 12(5), 769, doi:10.3390/rs12050769, 2020.

O'Dell, K., Ford, B., Fischer, E. V. and Pierce, J. R.: Contribution of Wildland-Fire Smoke to US PM2.5 and Its Influence
on Recent Trends, Environmental Science & Technology, 53(4), 1797–1804, doi:10.1021/acs.est.8b05430, 2019.

520   Olfert, J. S. and Wang, J.: Dynamic Characteristics of a Fast-Response Aerosol Size Spectrometer, Aerosol Sci. Technol.,
43(2), 97–111, 2009.

Atmospheric
Chemistry
and Physics
Discussions

Onasch, T. B., Trimborn, A., Fortner, E. C., Jayne, J. T., Kok, G. L., Williams, L. R., Davidovits, P. and Worsnop, D. R.:
    Soot Particle Aerosol Mass Spectrometer: Development, Validation, and Initial Application, Aerosol Science and
    Technology, 46(7), 804–817, doi:10.1080/02786826.2012.663948, 2012.

525 Petters, M. D. and Kreidenweis, S. M.: A single parameter representation of hygroscopic growth and cloud condensation
    nucleus activity, Atmos. Chem. Phys., 7(8), 1961–1971, 2007.

Petters, M. D., Carrico, C. M., Kreidenweis, S. M., Prenni, A. J., DeMott, P. J., Collett, J. L. and Moosmüller, H.: Cloud
    condensation nucleation activity of biomass burning aerosol, J. Geophys. Res. D: Atmos., 114(22), 22205, 2009.

Ramnarine, E., Kodros, J. K., Hodshire, A. L., Lonsdale, C. R., Alvarado, M. J. and Pierce, J. R.: Effects of near-source
530   coagulation of biomass burning aerosols on global predictions of aerosol size distributions and implications for
    aerosol radiative effects, Atmos. Chem. Phys., 19(9), 6561–6577, 2019.

Reid, C. E., Brauer, M., Johnston, F. H., Jerrett, M., Balmes, J. R. and Elliott, C. T.: Critical review of health impacts of
    wildfire smoke exposure, Environmental Health Perspectives, 124(9), 1334–1343, doi:10.1289/ehp.1409277, 2016.

Reid, J. S., Hobbs, P. V., Ferek, R. J., Blake, D. R., Martins, J. V., Dunlap, M. R. and Liousse, C.: Physical, chemical, and
535   optical properties of regional hazes dominated by smoke in Brazil, J. Geophys. Res. D: Atmos., 103(D24), 32059–
    32080, 1998.

Reid, J. S., Eck, T. F., Christopher, S. A., Koppmann, R., Dubovik, O., Eleuterio, D. P., Holben, B. N., Reid, E. A. and
    Zhang, J.: A review of biomass burning emissions part III: intensive optical properties of biomass burning particles,
    Atmos. Chem. Phys., 5, 827–849, 2005.

540 Sakamoto, K. M., Allan, J. D., Coe, H., Taylor, J. W., Duck, T. J. and Pierce, J. R.: Aged boreal biomass-burning aerosol
    size distributions from BORTAS 2011, Atmos. Chem. Phys., 15(4), 1633–1646, 2015.

Sakamoto, K. M., Laing, J. R., Stevens, R. G., Jaffe, D. A. and Pierce, J. R.: The evolution of biomass-burning aerosol size
    distributions due to coagulation: Dependence on fire and meteorological details and parameterization, Atmos.
    Chem. Phys., 16(12), 7709–7724, 2016.

545 Schwarz, J. P., Gao, R. S., Fahey, D. W., Thomson, D. S., Watts, L. A., Wilson, J. C., Reeves, J. M., Darbeheshti, M.,
    Baumgardner, D. G., Kok, G. L. and Others: Single-particle measurements of midlatitude black carbon and light-
    scattering aerosols from the boundary layer to the lower stratosphere, J. Geophys. Res. D: Atmos., 111(D16)
    [online] Available from: https://agupubs.onlinelibrary.wiley.com/doi/abs/10.1029/2006JD007076, 2006.

Sedlacek, A. J., Iii, Buseck, P. R., Adachi, K., Onasch, T. B., Springston, S. R. and Kleinman, L.: Formation and evolution
550   of Tar Balls from Northwestern US wildfires, Atmos. Chem. Phys. Discuss., (Figure 1), 1–28, 2018.

Seinfeld, J. H. and Pandis, S. N.: Atmospheric chemistry and physics: From air pollution to climate change, John Willey &
    Sons, Inc. , New York, 2006.

Shrivastava, M., Cappa, C. D., Fan, J., Goldstein, A. H., Guenther, A. B., Jimenez, J. L., Kuang, C., Laskin, A., Martin, S.
    T., Ng, N. L. and Others: Recent advances in understanding secondary organic aerosol: Implications for global
555   climate forcing, Rev. Geophys., 55(2), 509–559, 2017.

Spracklen, D. V., Mickley, L. J., Logan, J. A., Hudman, R. C., Yevich, R., Flannigan, M. D. and Westerling, A. L.: Impacts of climate change from 2000 to 2050 on wildfire activity and carbonaceous aerosol concentrations in the western United States, J. Geophys. Res., 114(D20), 1418, 2009.

Tang, X., Madronich, S., Wallington, T. and Calamari, D.: Changes in tropospheric composition and air quality, J.
560   Photochem. Photobiol. B, 46(1-3), 83–95, 1998.

Tie, X.: Effect of clouds on photolysis and oxidants in the troposphere, J. Geophys. Res., 108(D20), 23,073, 2003.

Twomey, S.: Pollution and the planetary albedo, Atmos. Environ., 8(12), 1251–1256, 1974.

Vakkari, V., Kerminen, V.-M., Beukes, J. P., Titta, P., van Zyl, P. G., Josipovic, M., Wnter, A. D., Jaars, K., Worsnop, D. R., Kulmala, M. and Laakso, L.: Rapid changes in biomass burning aerosols by atmospheric oxidation, Geophys.
565   Res. Lett., 2644–2651, 2014.

Vakkari, V., Beukes, J. P., Dal Maso, M., Aurela, M., Josipovic, M. and van Zyl, P. G.: Major secondary aerosol formation in southern African open biomass burning plumes, Nat. Geosci., 11(8), 580–583, 2018.

Volkamer, R., Jimenez, J. L., San Martini, F., Dzepina, K., Zhang, Q., Salcedo, D., Molina, L. T., Worsnop, D. R. and Molina, M. J.: Secondary organic aerosol formation from anthropogenic air pollution: Rapid and higher than
570   expected, Geophys. Res. Lett., 33(17), 4407, 2006.

Volkamer, R., Ziemann, P. J. and Molina, M. J.: Secondary Organic Aerosol Formation from Acetylene (C2H2): seed effect on SOA yields due to organic photochemistry in the aerosol aqueous phase, Atmos. Chem. Phys., 9(6), 1907–1928, 2009.

Wang, J., -N. Lee, Y., Daum, P. H., Jayne, J. and Alexander, M. L.: Effects of aerosol organics on cloud condensation
575   nucleus (CCN) concentration and first indirect aerosol effect, Atmospheric Chemistry and Physics, 8(21), 6325–6339, doi:10.5194/acp-8-6325-2008, 2008.

Yang, M., Blomquist, B. W. and Huebert, B. J.: Constraining the concentration of the hydroxyl radical in a stratocumulus-topped marine boundary layer from sea-to-air eddy covariance flux measurements of dimethylsulfide, Atmos. Chem. Phys., 9(23), 9225–9236, 2009.

580   Yokelson, R. J., Crounse, J. D., DeCarlo, P. F., Karl, T., Urbanski, S., Atlas, E., Campos, T., Shinozuka, Y., Kapustin, V., Clarke, A. D., Weinheimer, A., Knapp, D. J., Montzka, D. D., Holloway, J., Weibring, P., Flocke, F., Zheng, W., Toohey, D., Wennberg, P. O., Wiedinmyer, C., Mauldin, L., Fried, A., Richter, D., Walega, J., Jimenez, J. L., Adachi, K., Buseck, P. R., Hall, S. R. and Shetter, R.: Emissions from biomass burning in the Yucatan, Atmos. Chem. Phys., 9(15), 5785–5812, 2009.

585   Yue, X., Mickley, L. J., Logan, J. A. and Kaplan, J. O.: Ensemble projections of wildfire activity and carbonaceous aerosol concentrations over the western United States in the mid-21st century, Atmospheric Environment, 77, 767–780, doi:10.1016/j.atmosenv.2013.06.003, 2013.

Zhou, S., Collier, S., Jaffe, D. A., Briggs, N. L., Hee, J., Sedlacek, A. J., III, Kleinman, L., Onasch, T. B. and Zhang, Q.:
Regional influence of wildfires on aerosol chemistry in the western US and insights into atmospheric aging of
590   biomass burning organic aerosol, Atmos. Chem. Phys., 17(3), 2477–2493, 2017.
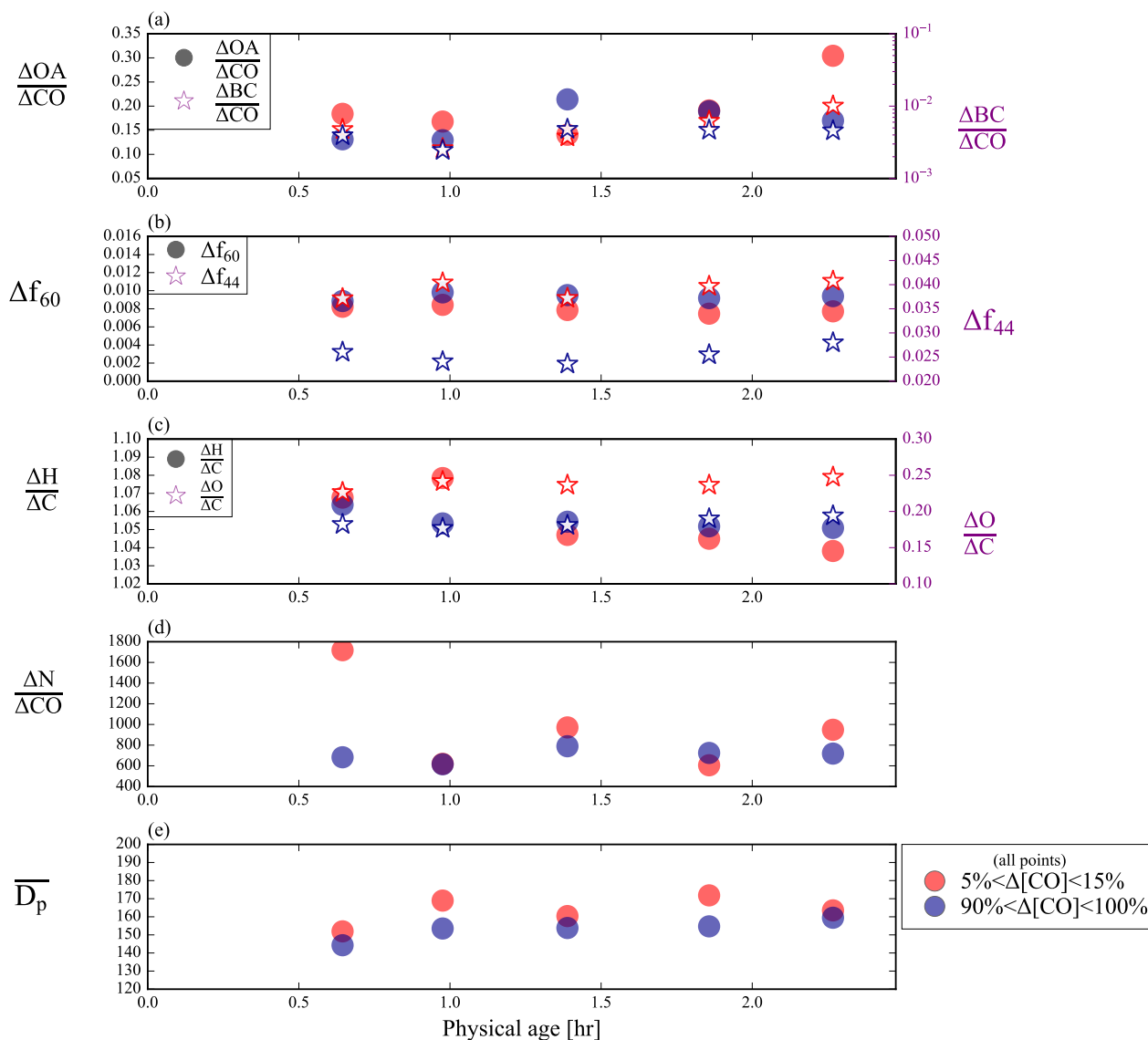
Figure 1: Aerosol properties from the first set of pseudo-Lagrangian transects from the Colockum fire on flight '730b' (a)
ΔOA/ΔCO (right y-axis) and ΔrBC/ΔCO (left y-axis), (b) Δf$_{60}$ (right y-axis) and Δf$_{44}$ (left y-axis), (c) ΔH/ΔC (right y-axis) and

$\Delta O/\Delta C$ (left y-axis), (d) $\Delta N/\Delta CO$, and (e) $\overline{D_p}$ against physical age. For each transect, the data is divided into edge (the lowest 5-15% of ΔCO data; red points) and core (90-100% of ΔCO data; blue points). $\Delta rBC/\Delta CO$ is shown in log scale to improve clarity.

600
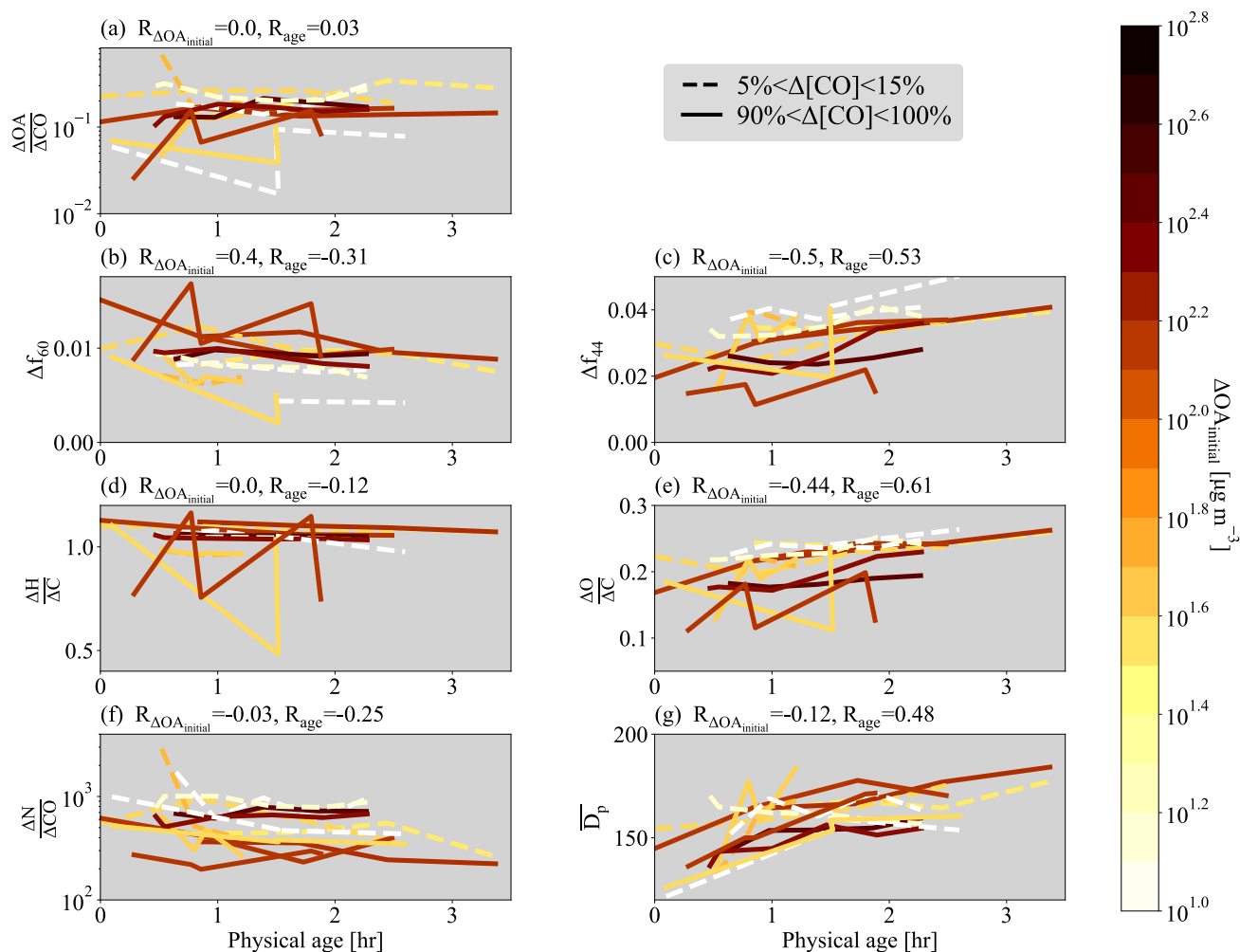
Figure 2. Various normalized parameters as a function of age for the 7 sets of pseudo-Lagrangian transects. Separate lines are shown for the edges (lowest 5-15% of ΔCO; dashed lines) and cores (highest 90-100% of ΔCO; solid lines). (a) $\Delta OA/\Delta CO$, (b) Δf_{60}, (c) Δf_{44}, (d) $\Delta H/\Delta C$, (e) $\Delta O/\Delta C$, (f) $\Delta N_{40\text{-}262\ nm}/\Delta CO$, and (g) $\overline{D_p}$ between 40-262 nm against physical age for all flights, colored by $\Delta OA_{initial}$. Some flights have missing data. Also provided is the Spearman correlation coefficient, R, between each variable and $\Delta OA_{initial}$ and physical age for each variable. Note that panels (a), (d), and (g) have a log y-axis.

610
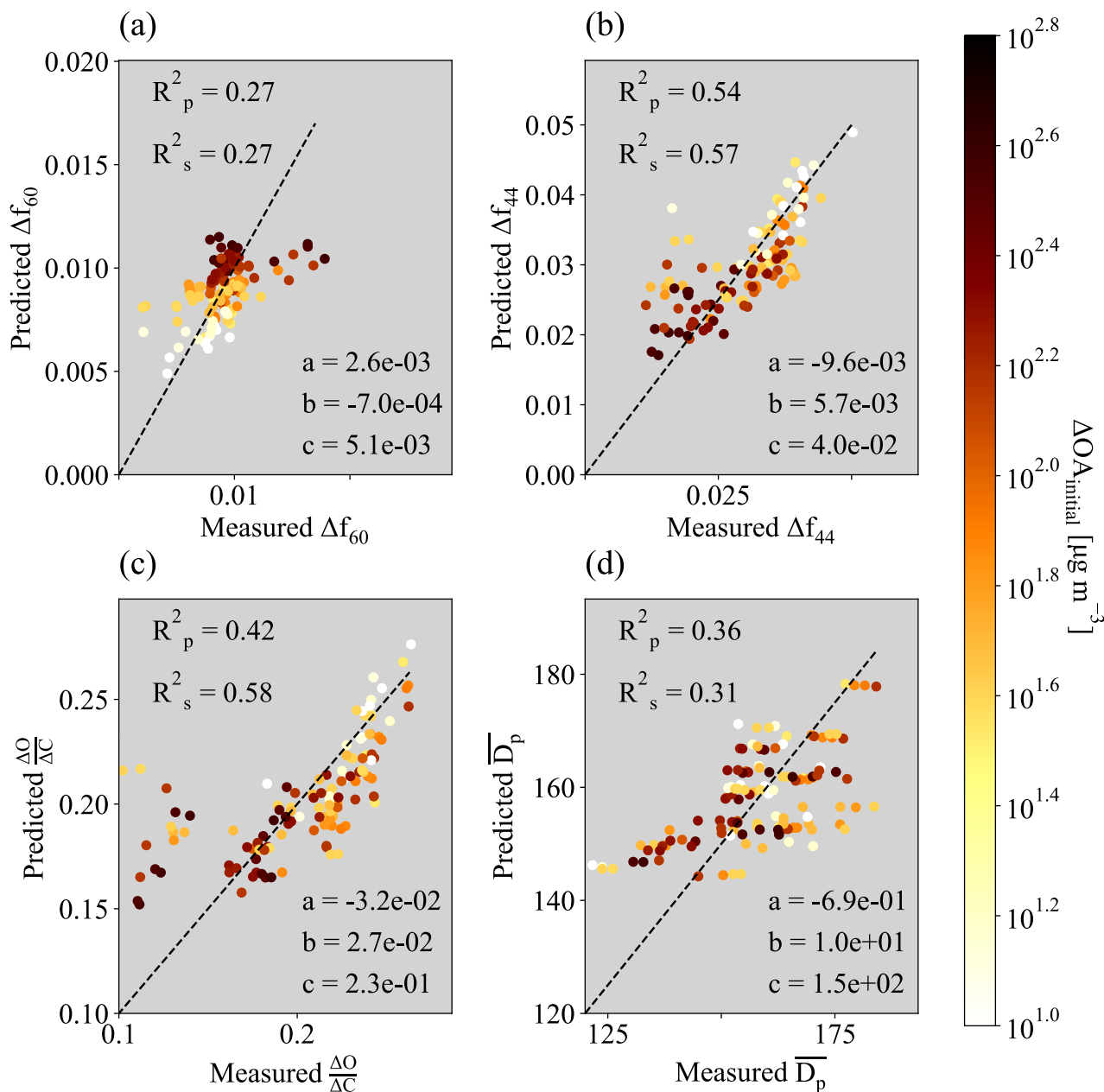
Figure 3. Measured versus predicted (a) Δf_{60}, (b) Δf_{44}, (c) $\Delta O/\Delta C$, and (d) $\overline{D_p}$ between 40-262 nm. The predicted values are from the equation $X = a\ log_{10}(OA_{initial}) + b\ (Physical\ age) + c$ where $X = \Delta f_{60}$, Δf_{44}, $\Delta O/\Delta C$, or $\overline{D_p}$. The values of *a*, *b*, and *c* are provided within each subpanel, as are the Pearson and Spearman coefficients of determination (R^2_p and R^2_s, respectively). Note that Fig. 2 provides R values rather than R^2 to provide information upon the trend of the correlation. Included in the fit and figure are points from all four ΔCO regions within the plume (the 5-15%, 15-50%, 50-90%, and 90-100% of ΔCO), all colored by the mean $\Delta OA_{initial}$ of each ΔCO percentile range.

615